

Supplemental Material for
Robust ferromagnetism in two-dimensional GeC/CrN heterobilayer

TABLE SI: Structural parameters of the GeC/CrN heterostructure. The lattice constant (a), interlayer distance (d), buckling parameter ($\delta_{GeC(CrN)}$), binding energy (E_b) and charge transfer between CrN and GeC layers (ΔQ), net magnetization (M), Hubbard U parameters.

system	d (Å)	E_b (eV/atom)	ΔQ ($ e $)	M (μ_B /per Cr atom)	U (eV)
$\sqrt{7}$ ($\theta_{TW} = 38.7^\circ$)	3.13	0.069	0.0665	3.0	4
$\sqrt{13}$ ($\theta_{TW} = 28.3^\circ$)	3.14	0.072	0.0564	3.0	4
$\sqrt{19}$ ($\theta_{TW} = 47.5^\circ$)	3.05	0.069	0.1034	3.0	4
AA	3.24	0.050	0.0183	3.0	4.2
AB	3.25	0.064	0.0162	3.0	3.8
AA*	2.84	0.099	0.0195	3.0	4.2
AB*	2.79	0.100	0.0646	2.8	3.8

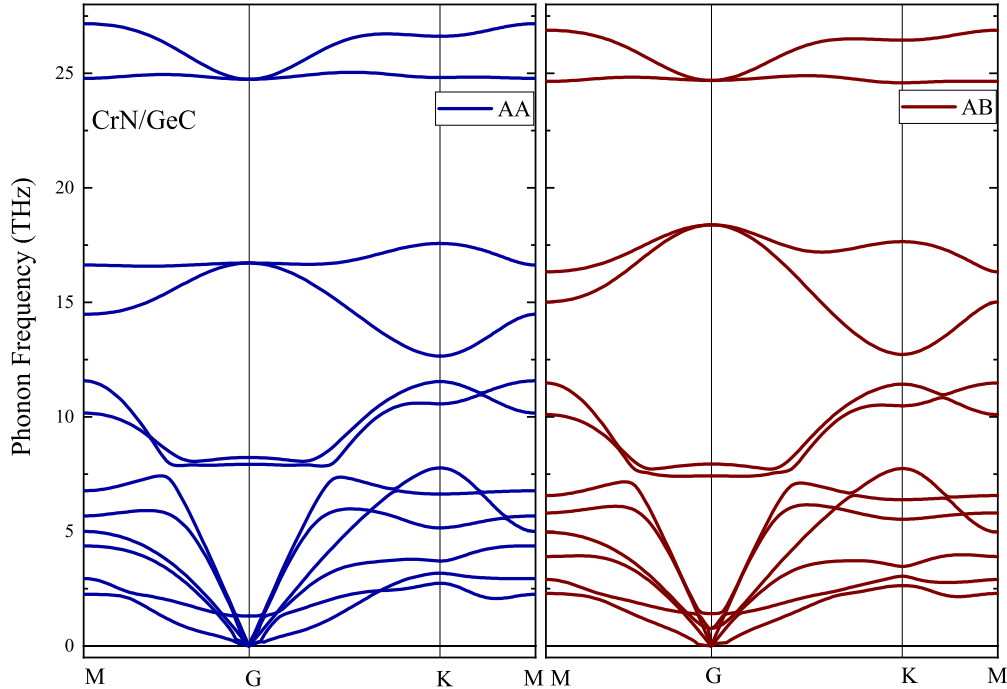


FIG. S1: The phonon spectra of (a) AA and (b) AB stackings of GeC/CrN

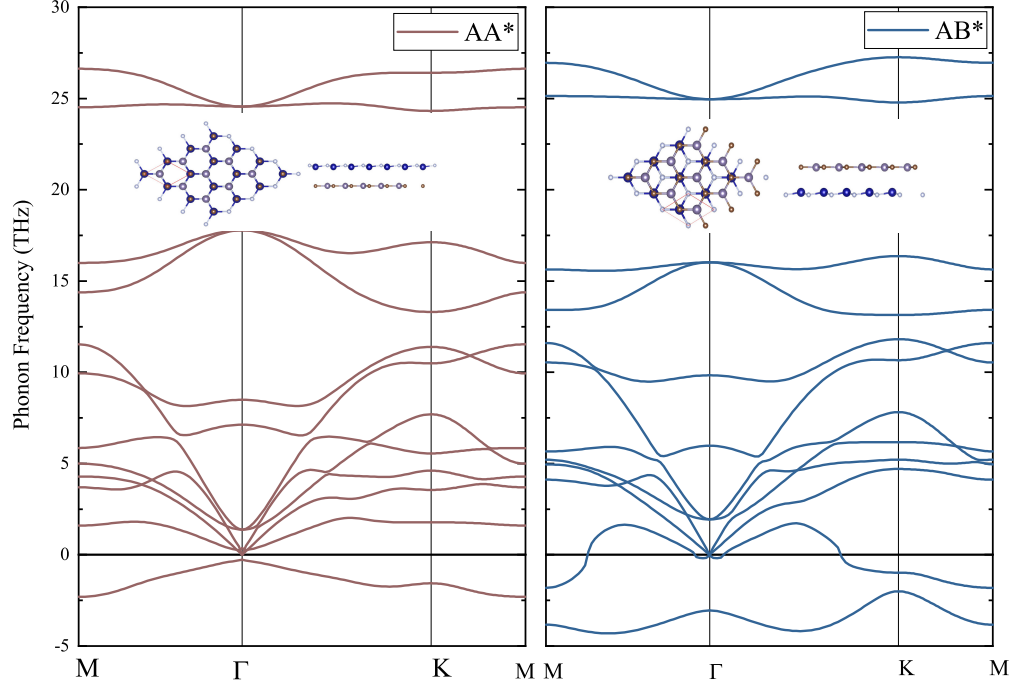


FIG. S2: The phonon spectra of (a) AA* and (b) AB* (unstable stackings) of GeC/CrN

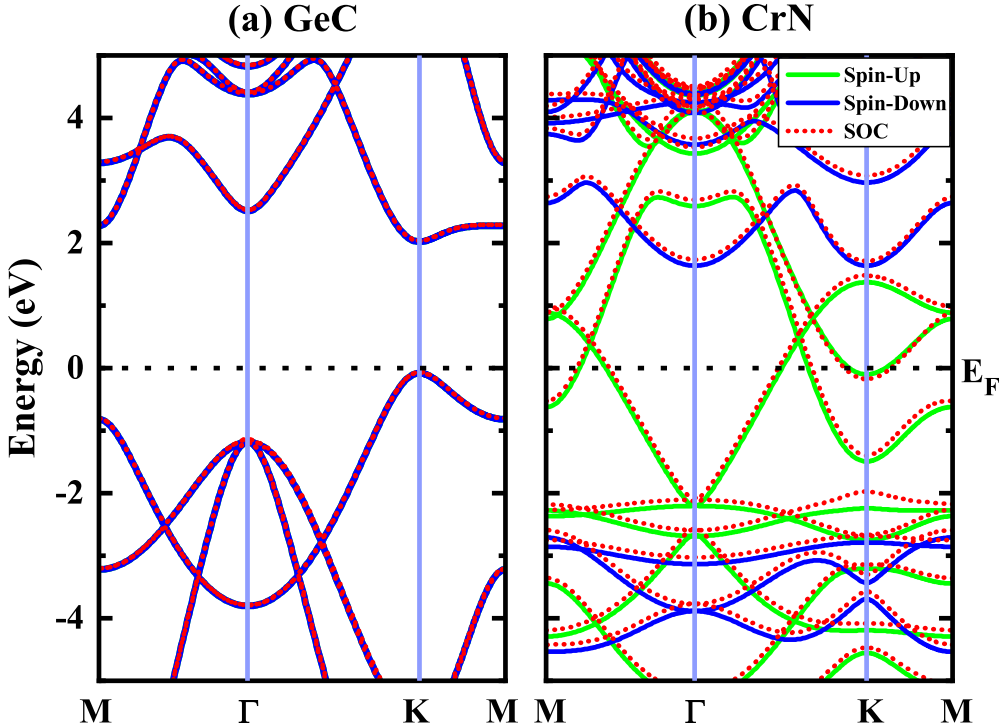


FIG. S3: The energy band spectrum of pristine (a) GeC monolayer and (b) CrN monolayer. The Fermi level is set to be zero.

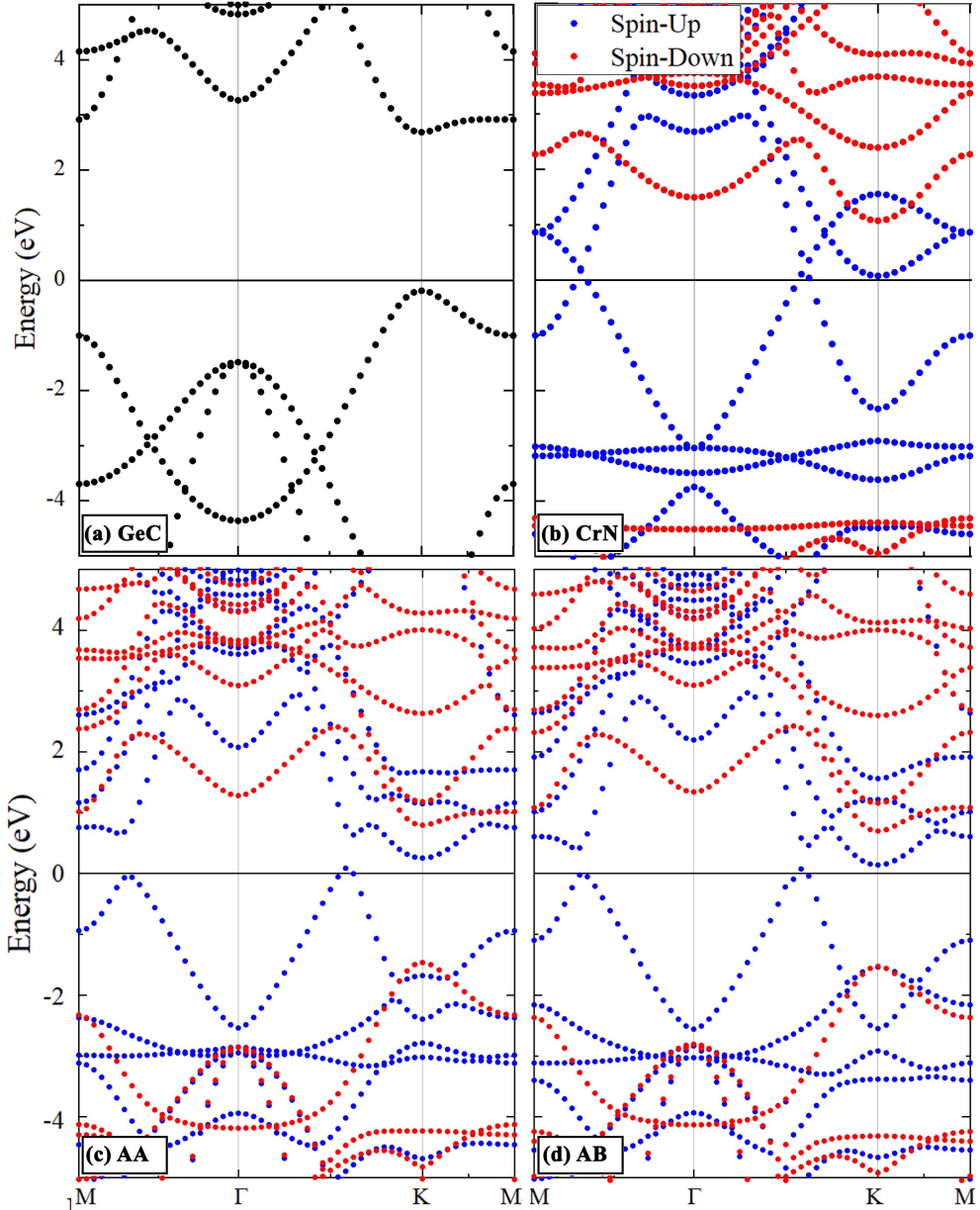


FIG. S4: The energy band spectrum of (a) GeC monolayer and (b) CrN monolayer, (c) AA and (d) AB for HSE06. The Fermi level is set to be zero.

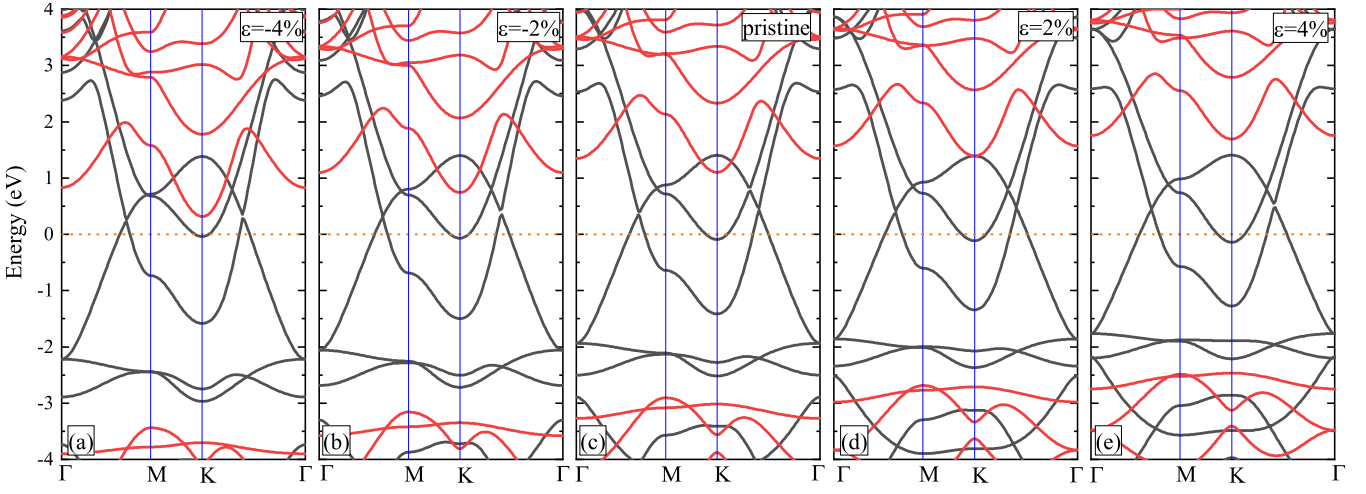


FIG. S5: The band spectrum of monolayer CrN under biaxial strain. The Fermi level is set to be zero.

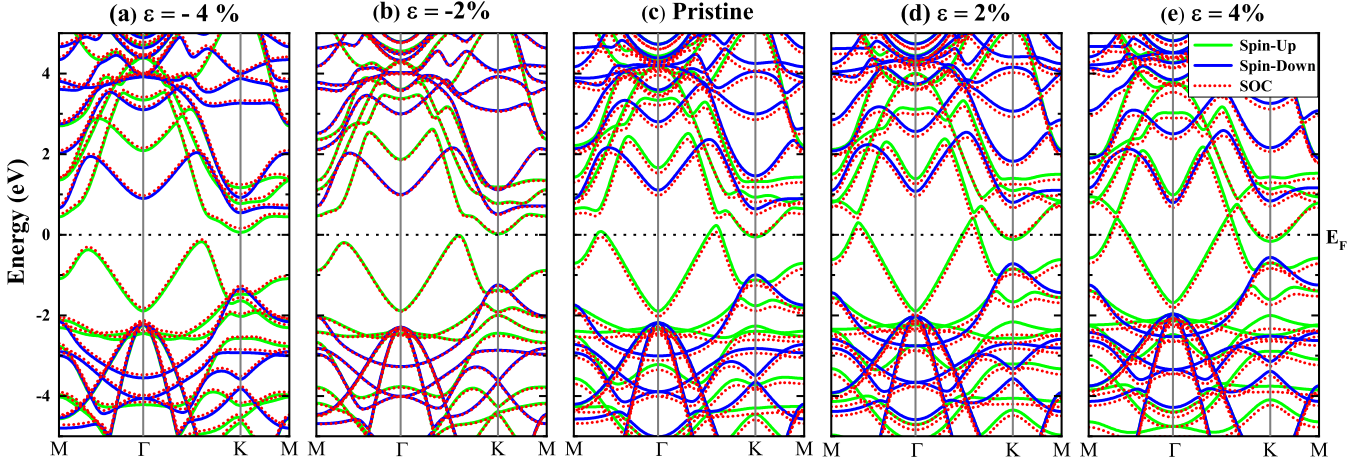


FIG. S6: The band structure of AA for (a) $\varepsilon=-4\%$, (b) $\varepsilon=-2\%$ under compressive strain, (c) pristine, (d) $\varepsilon=2\%$, and (e) $\varepsilon=4\%$ under tensile strain. The Fermi level is set to be zero.

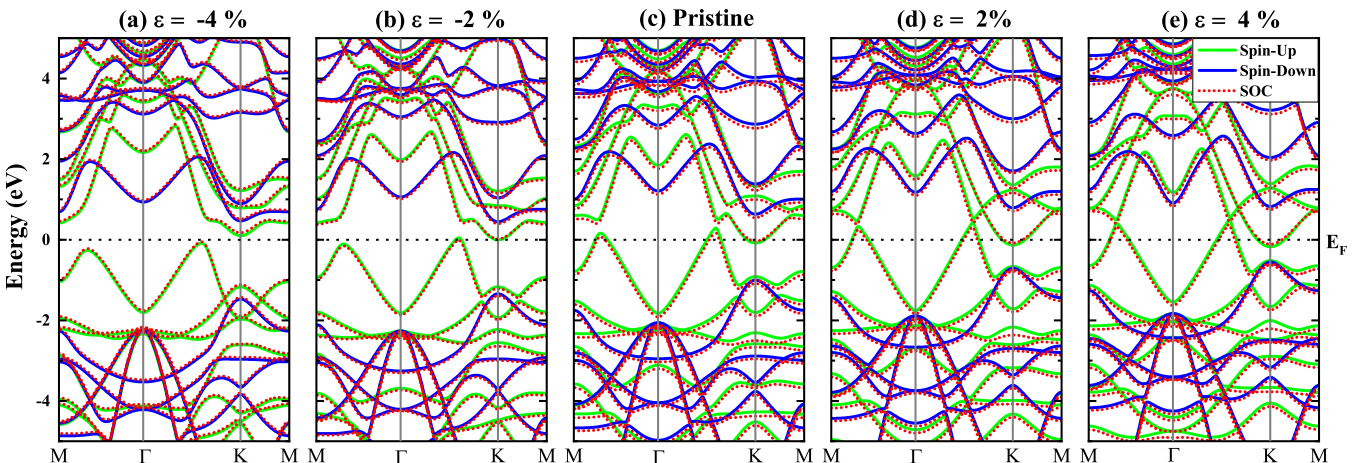


FIG. S7: The band structure of AB for (a) $\varepsilon=-4\%$, (b) $\varepsilon=-2\%$ under compressive strain, (c) pristine, (d) $\varepsilon=2\%$, and (e) $\varepsilon=4\%$ under tensile strain. The Fermi level is set to be zero.

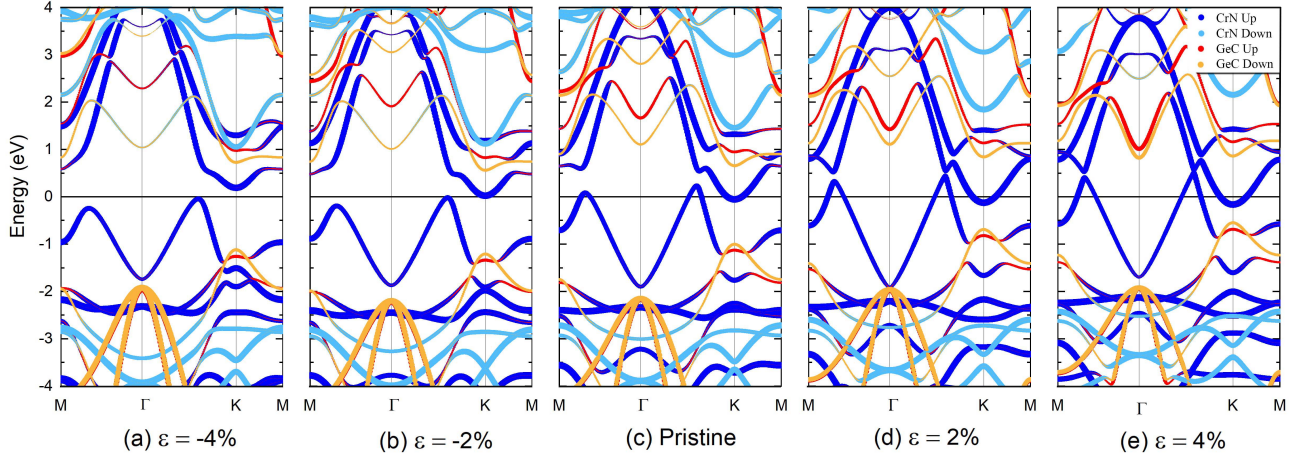


FIG. S8: The partial band structure of AA for (a) $\varepsilon = -4\%$, (b) $\varepsilon = -2\%$ under compressive strain, (c) pristine, (d) $\varepsilon = 2\%$, and (e) $\varepsilon = 4\%$ under tensile strain. The Fermi level is set to be zero.

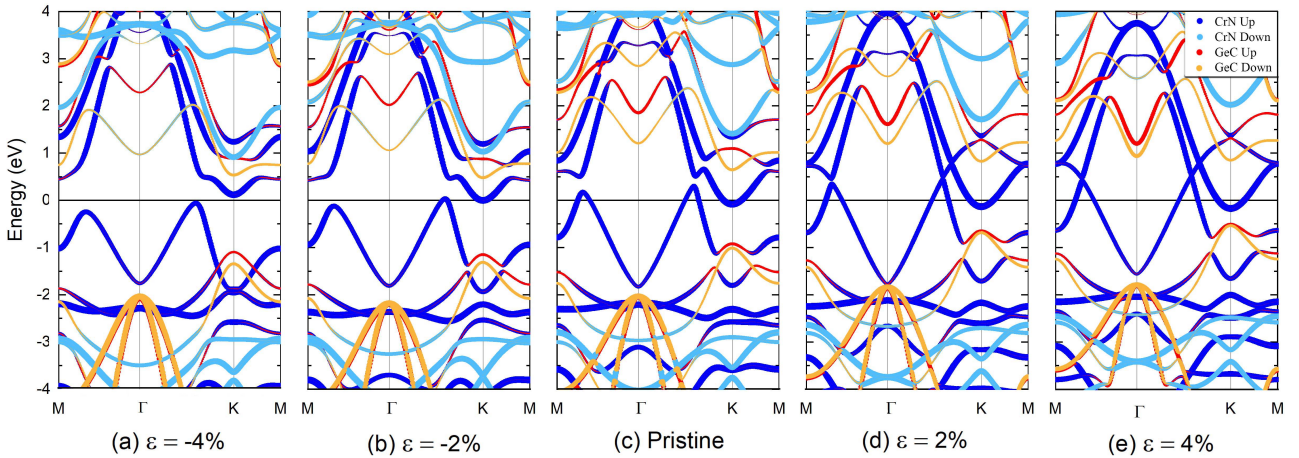


FIG. S9: The partial band structure of AB for (a) $\varepsilon = -4\%$, (b) $\varepsilon = -2\%$ under compressive strain, (c) pristine, (d) $\varepsilon = 2\%$, and (e) $\varepsilon = 4\%$ under tensile strain. The Fermi level is set to be zero.

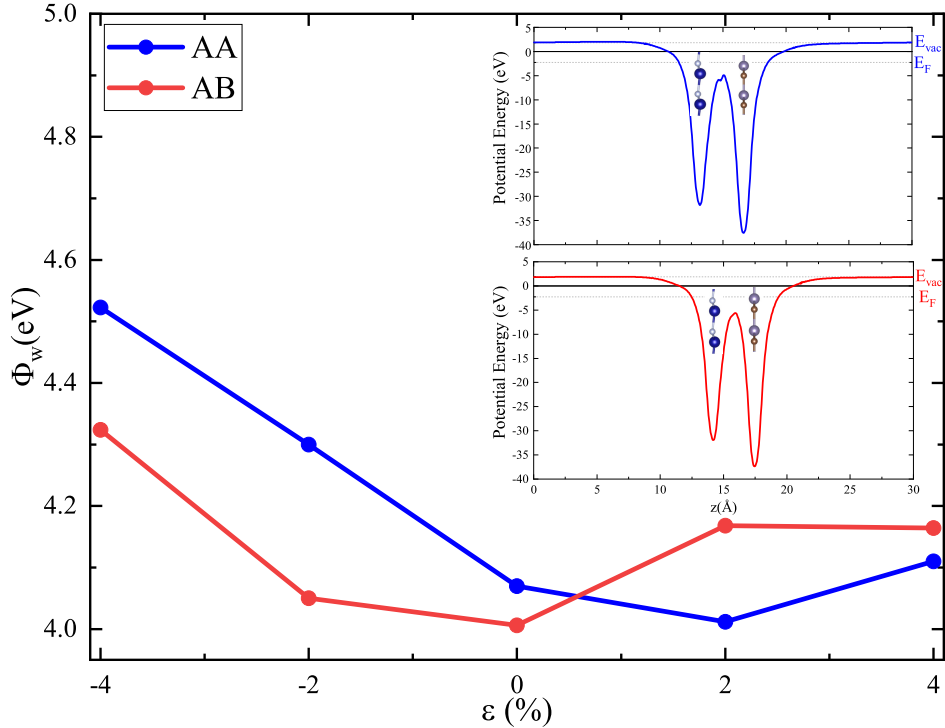


FIG. S10: The calculated work function (Φ_w) of GeC/CrN heterobilayers as a function of strain. Inset: Electrostatic potential energy of AA and AB. The Fermi and the vacuum energies are marked on the potential energy figure.

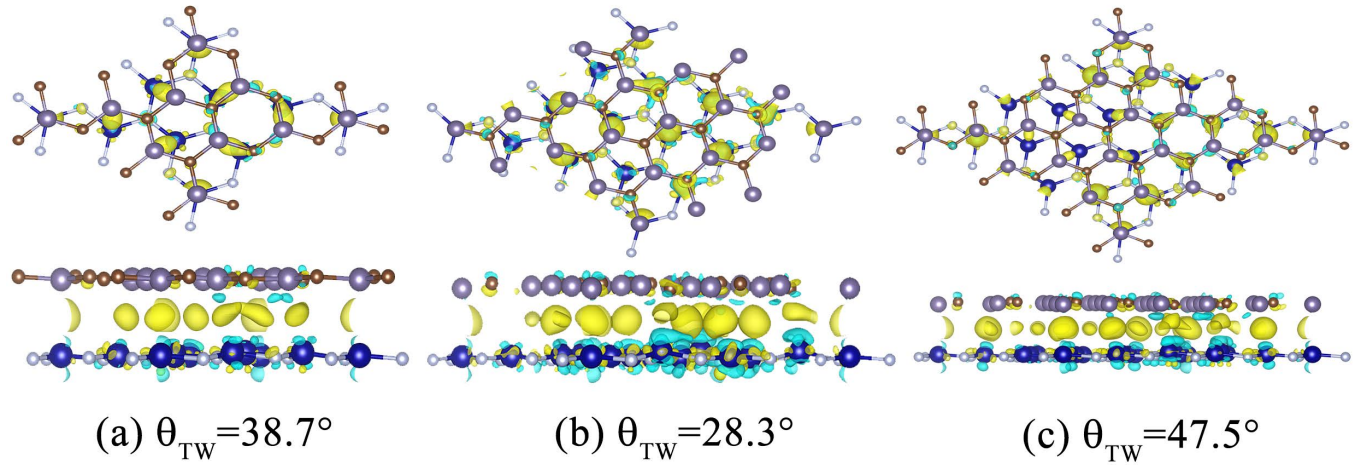


FIG. S11: The charge density differences for (a) $\theta_{TW} = 38.7^\circ$, (b) $\theta_{TW} = 28.3^\circ$ and (c) $\theta_{TW} = 47.5^\circ$ of twisted GeC/CrN heterobilayer. The isosurface value is set to be $0.0015 \text{ e}\text{\AA}^{-3}$ for all figures.

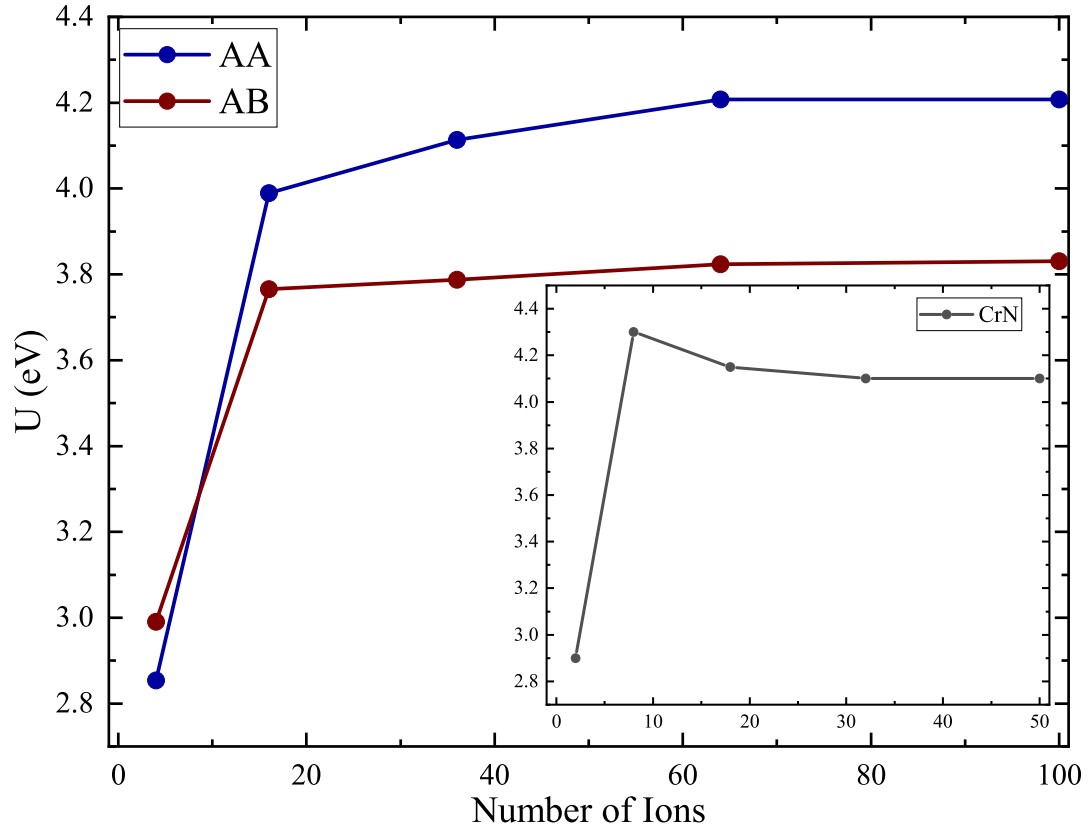


FIG. S12: The calculated Hubbard (U) parameters of AA, AB, and CrN monolayer by using the linear response theory.